Hydrophobic Effect on Alkaline Stability of Graft Chains in Ammonium-type Anion Exchange Membranes Prepared by Radiation-Induced Graft Polymerization

Takashi Hamada, *[a]† Yue Zhao, [a] Kimio Yoshimura, [a] Aurel Radulescu, [b] Kenji Ohwada, [c] and Yasunari Maekawa *[a]

[a] Dr. Takashi Hamada,[†] Dr. Yue Zhao, Dr. Kimio Yoshimura, and Dr. Yasunari Maekawa Department of Advanced Functional Materials Research, Takasaki Advanced Radiation Research Institute, Quantum Beam Science Research Directorate, National Institutes for Quantum and Radiological Science and Technology (QST), 1233 Watanuki, Takasaki, Gunma 370-1292, Japan

† Present address:

Dr. Takashi Hamada

Graduate School of Advanced Science and Engineering, Hiroshima University, 1-4-1 Kagamiyama, Higashi-Hiroshima, Hiroshima 739-8527, Japan

E-mail: hama@hiroshima-u.ac.jp

[b] Dr. Aurel Radulescu

Forschungszentrum Jülich GmbH, Jülich Centre for Neutron Science@MLZ, Lichtenbergstraße 1, D-85747 Garching, Germany

[c] Dr. Kenji Ohwada

Synchrotron Radiation Research Center, Quantum Beam Science Research Directorate, National Institutes for Quantum and Radiological Science and Technology (QST), 1-1-1 Kouto, Sayo, Hyogo 679-5148, Japan

Corresponding authors: Takashi Hamada and Yasunari Maekawa E-mail: hama@hiroshima-u.ac.jp and maekawa.yasunari@qst.go.jp

Abstract

Vinylbenzyltrimethylammonium hydroxide (VBA) and styrene (St) cografted poly(ethylene-co-tetrafluoroethylene) anion exchange membranes (VBA/St-AEM) were prepared by the radiation-induced graft polymerization of chloromethylstyrene and St and sequential quaternization and anion exchange reactions. Increasing the St content in the grafts to 63% resulted in a gradual 21% and 34% decrease in the conductivity and water uptake, respectively, compared to those in the VBA-homo-grafted AEM. AEMs with a higher St content (81%) showed a 9% and 18% higher conductivity and water uptake, respectively. Small-angle neutron scattering showed that the sudden growth of "water puddles" consisting of water-rich nanodomains dispersed randomly in phase-separated hydrophilic ion channels enhanced the

conductivity and water uptake. In the alkaline durability test of VBA/St-AEM in 1 M potassium hydroxide at 80 °C for 720 h, the loss of the conductivity was suppressed from 43% to 8%, when the St contents in the grafts were increased from 0% to 63%.

1. Introduction

Anion exchange membranes (AEMs) have attracted considerable attention because nonprecious metals, such as nickel, cobalt, and iron, can be used to prepare anion exchange membrane fuel cells instead of expensive platinum. However, compared to proton exchange membranes (PEMs), AEMs have several issues, such as lower power-generation efficiency, low durability, and mechanical stability. [5-7] In particular, the chemical stability of AEMs can be improved under alkaline conditions. Many researchers have focused on AEMs consisting of quaternary alkylammonium^[8-10] and imidazolium^[11-15] groups. Unfortunately, solving the chemical stability in alkaline solution at a high temperature (80 °C) is still a challenge. Understanding the degradation mechanisms of AEMs in alkaline solutions is important for improving their chemical stability. On the other hand, there are still limited examples to reveal the degradation mechanism of AEMs. For example, hydroxide ions attack benzyltrimethylammonium and imidazolium cations to produce benzyl alcohol and ring-opening products in alkaline solutions at high temperatures, respectively. Moreover, AEMs with hydrogen atoms at the β -positions from nitrogen atoms of ammonium and imidazolium groups are subjected to the Hoffmann elimination reaction in alkaline solutions at high temperatures.[16-20] Although base polymers should be important components to improve the chemical stability of AEMs, [21-24] it is important to improve their alkaline stability; hence, ionic groups should be designed.

One promising method to improve the durability to alkaline environments is incorporating a hydrophobic alkyl spacer next to the ionic groups. Hibbs et al. reported improvements in alkaline stability when the ionic groups are separated from the polymer backbone by an alkyl spacer.^[25] The conductivity of poly(phenylene)-based AEMs was decreased by 33% after

immersion in 4 M aqueous potassium hydroxide (KOH) for two weeks at 90 °C. In contrast, poly(phenylene)-based AEM with an alkyl spacer decreased by only 5% under the same conditions, i.e., the alkaline stability of poly(phenylene)-based AEM was enhanced by introducing an alkyl spacer. Wan et al. reported a spindle-shaped AEM based on poly(arylene ether ketone) having quaternary ammonium hydroxide via a hexyl side chain. The spindle-shaped AEM retained 64.8% of its initial conductivity after immersion in a 1 M sodium hydroxide (NaOH) solution for 15 days at 60 °C. The alkyl side chain between the polymer backbone and quaternary ammonium hydroxide improved the alkaline stability. Bae et al. synthesized polystyrene-*b*-poly(ethylene-*co*-butylene)-*b*-polystyrene triblock copolymers functionalized with alkyl-substituted quaternary ammonium groups and compared various cations on the vinyl polymer backbone: trimethyl, piperazine, dicylcohexyl, diisopropyl, and hexyl moieties. These AEMs remained chemically stable for four weeks in 1 M aqueous NaOH at 60 °C and 80 °C.

The authors have concentrated on developing graft-type PEMs and AEMs by radiation-induced graft polymerization. The advantage of radiation-induced graft polymerization is the introduction of ionic groups containing graft polymers into mechanically and thermally tough polymers, such as poly(ethylene-*co*-tetrafluoroethylene) (ETFE) and poly(ether ether ketone), while maintaining these properties. Therefore, these graft-type PEMs and AEMs composed of a mechanically and thermally tough crystalline substrate and ionic grafts will solve the problem of low alkaline stability. A previous study reported alkylammonium-containing membranes, poly(vinylbenzyltrimethylammonium hydroxide)-grafted ETFE (VBA-AEM), with ion-exchange capacities (IECs) of 1.35–2.35 mmol/g. VBA-AEM with a high IEC broke into several pieces after only three days in 1M KOH at 80 °C. Stable AEMs with a high water uptake (WU) of 127% did not maintain their shape in 10 M NaOH at 60 °C. The high basicity of

tetramethylammonium hydroxide might cause the decomposition of ETFE or the grafted chains.

The IEC affects the conductivity, WU, and dimensional stability. Previously reported VBA-AEMs with IECs of 1.35–2.35 mmol/g have a high WU, leading to low alkaline stability caused by the nucleophilic attack of hydroxide ions. As mentioned above, introducing hydrophobic alkyl groups is an effective way to improve the alkaline stability. The ionic groups are separated from the polymer backbone by a long alkyl spacer and are sterically crowded with a long alkyl chain. Thus, the introduction of hydrophobic groups to graft chains would improve the alkaline stability of graft-type AEM. On the other hand, the effects of hydrophobic substitutes in the grafts have not been investigated systematically for VBA-AEMs.

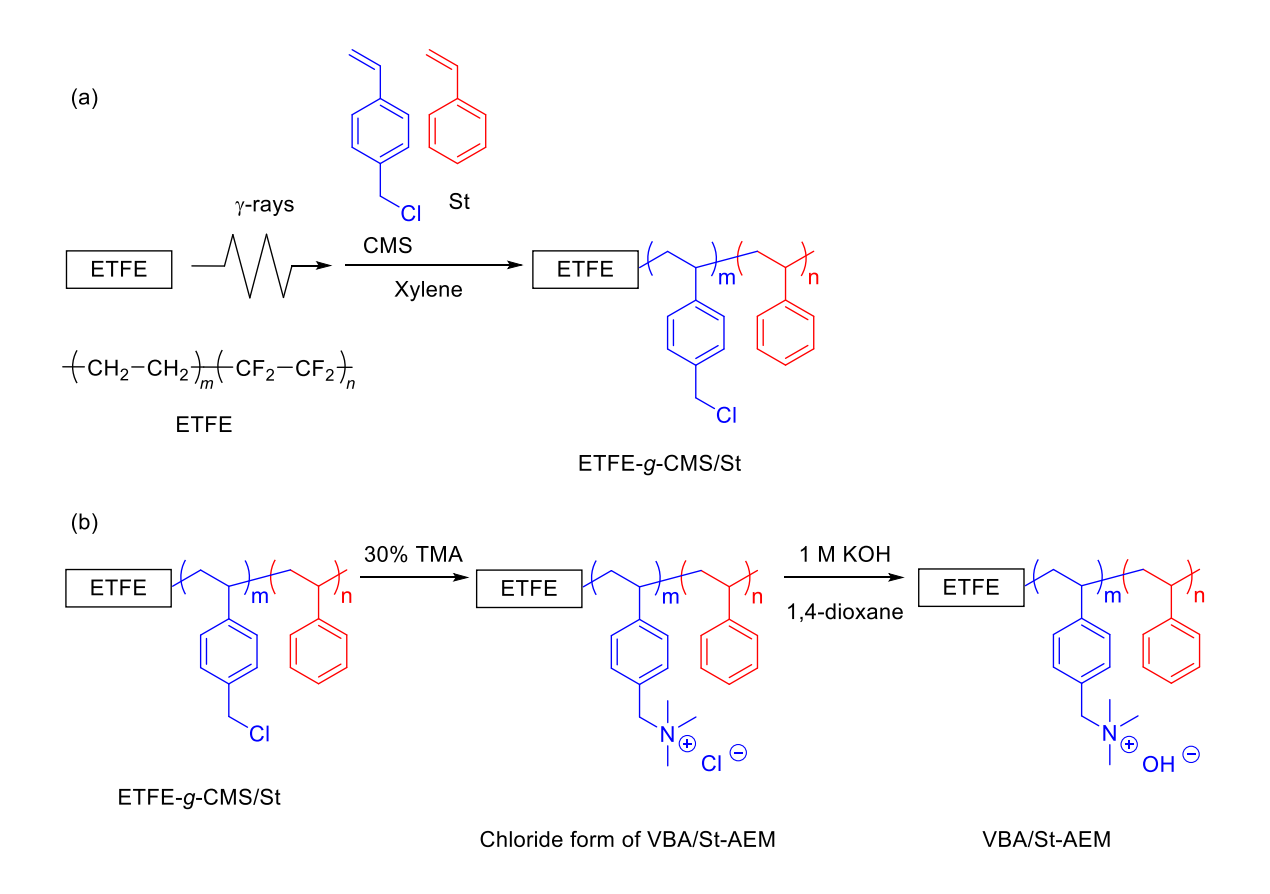
This paper reports the synthesis of poly(vinylbenzyltrimethylammonium hydroxide-co-styrene)-grafted ETFE membrane (VBA/St-AEM) by the radiation-induced graft polymerization of chloromethylstyrene (CMS) and styrene (St), followed by quaternization and ion-exchange reactions. To understand the effects of hydrophobic St in the graft chain, this study examined the conductivity, WU, mechanical property, and alkaline stability of AEM in 1 M KOH at 80 °C as a function of the St contents in the AEMs. Furthermore, the microscopic structures of VBA/St-AEM equilibrated in water were also investigated by small-angle neutron scattering (SANS).

2. Results and discussion

2.1. Preparation and characterization of graft-type AEMs

The ETFE films were pre-irradiated with 10–30 kGy in the presence of nitrogen gas at room temperature, according to the procedure reported elsewhere. Subsequently, the films were immersed in a 50 vol% solution of CMS and St in xylene or neat at 60 °C for 1–48 h. (Scheme 1 (a) and Table S1). Poly(chloromethylstyrene-co-styrene)-grafted ETFE (ETFE-g-CMS/St) with grafting degrees (GDs) of 31–153% was prepared by the radiation-induced graft

polymerization of CMS and St with varying volume ratios (CMS/St = 10/0, 8/2, 7/3, 5/5, 4/6, and 2/8). The molar ratio of CMS and St in the graft polymers could not be estimated simply by nuclear magnetic resonance (NMR) spectroscopy because the graft-type ETFE films prepared by radiation-induced graft polymerization were insoluble in organic solvents. Therefore, the estimated molar ratio of CMS and St will be discussed in detail in the characterization of the final AEMs.



Scheme 1. Preparation procedure of VBA/St-AEM. (a) Radiation-induced graft polymerization of CMS and St into the ETFE film; (b) Quaternization by TMA and ion-exchange reaction by KOH.

A previous study reported the quaternization of the ETFE-g-CMS in a 30% trimethylamine (TMA) aqueous solution at room temperature for 10 h to give

poly(vinylbenzyltrimethylammonium chloride)-grafted ETFE (the chloride form of VBA-AEM) in almost quantitative yield.¹⁵⁰ Given that the quaternization of ETFE-*g*-CMS/St proceeded quantitatively, the molar ratio of CMS and St in the graft chain could be estimated from the gravimetric changes before and after quaternization (see Supporting Information). When the quaternization of ETFE-*g*-CMS/St with GDs of 31–153% was conducted under the same conditions for 24 h (**Scheme 1 (b)**), the estimated molar ratios of CMS/St of the ETFE-*g*-CMS/St were 100/0, 91/9, 65/35, 46/54, 37/67, and 19/81 in the graft chain (**Table S2**). The chloride ion contents, i.e., a millimolar amount of chloride ions per 1 g of the dry chloride form of VBA/St-AEM (IEC₀), were estimated to be 0.94–1.33 mmol/g from the weight change (**Table S2**). The IEC₀ of VBA/St-AEM (Cl form) with different GDs were similar, which was advantageous in comparing the effects of St in the graft chain. The chloride form of VBA/St-AEM was converted to the hydroxide form to obtain the VBA/St-AEM.

The completion of quaternization of ETFE-*g*-CMS/St and ion-exchange reaction from the chloride to hydroxide form in VBA/St-AEM was confirmed by scanning electron microscopy–energy-dispersive X-ray spectroscopy (SEM-EDX) analysis of cross-sections of these membranes. The SEM-EDX spectrum of a cross-section of ETFE-*g*-CMS/St (5/5) with a GD of 43% indicated that chloride ions were distributed homogeneously in the grafted film; i.e., the graft polymerization of CMS proceeded in the perpendicular direction of the ETFE film. This behavior concurs with a previous report showing a homogeneous distribution of graft chains according to SEM-EDX.^[29]

A new peak at 2.63 eV corresponding to chloride atoms appeared in the SEM-EDX spectrum of ETFE-g-CMS/St (5/5) with a GD of 43%, along with fluorine, silicon, and gold atoms derived from the substrate and sample preparation (**Figure 1**). As shown in **Scheme 1** (b), there were no significant changes in the SEM-EDX spectra by quaternization. In particular, the peak for chloride atoms derived from the counter anion was also observed at 2.63 eV. The chlorine peak at 2.63 eV disappeared in the SEM-EDX spectrum of a cross-section of VBA/St-AEM

(5/5) with an IEC of 0.84 mmol/g, indicating the ion-exchange reaction proceeded very quickly and quantitatively in 3 h (**Figure 1**).

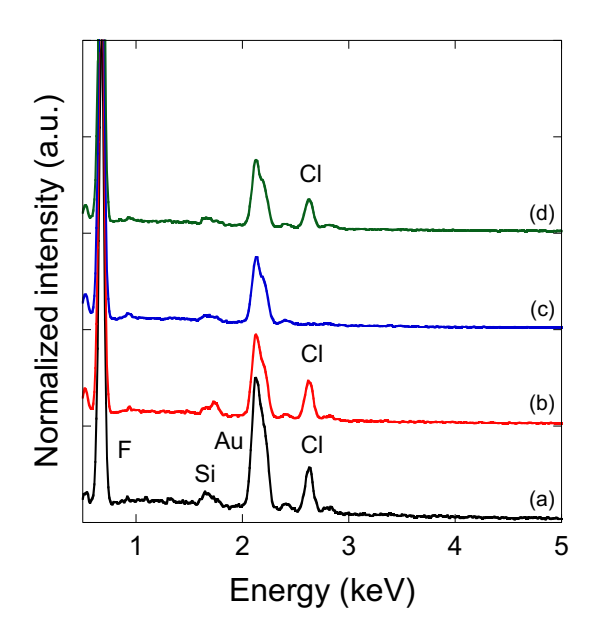


Figure 1. SEM-EDX spectra of (a) ETFE-*g*-CMS/St with a GD of 43%, (b) chloride form of VBA/St-AEM (5/5) with an IEC_a of 1.02 mmol/g, (c) VBA/St-AEM with an IEC of 0.84 mmol/g, and (d) chloride form of VBA/St-AEM (5/5) with an IEC_a of 1.03 mmol/g.

2.2. Electrolyte properties of graft-type AEMs

The chloride form of VBA-AEM and VBA/St-AEM with IEC_a values ranging from 0.94 to 1.33 mmol/g showed conductivities of 3.9–11 and 14–26 mS/cm at 20 °C and 60 °C, respectively (**Table S2**). The WU of the chloride form of VBA-AEM and VBA/St-AEM ranged from 11% to 19% at 20 °C (**Table S2**). The conductivities of VBA/St-AEM were measured in N₂ bubbled water because the hydroxide form of the AEM is converted quickly to the bicarbonate form in non-N₂ bubbled water (i.e., water containing dissolved CO₂). As shown in **Table 1**, VBA/St-AEM with IEC values ranging from 0.78 to 1.06 mmol/g showed conductivities of 45–59 and 70–97 mS/cm at 20 °C and 60 °C, respectively. The yields of the conversion of VBA/St-AEM from the chloride to hydroxide were 77–89% as determined by

titrimetric analysis, as shown in **Table 1**. In a previous paper, the conversion of VBA-AEM was 88–92%. Specifically, the IEC of the membrane was approximately 90% based on the expected IEC calculated using a millimolar amount of quaternary ammonium salt in a unit weight (1 g) of the AEM. However, the IECs of VBA/St-AEM were slightly lower than those of previously reported membranes, even though SEM-EDX did not show a chlorine peak. A possible explanation for the lower IEC may be the hydrophobicity of St in the graft chain that results in an incomplete ion-exchange reaction from hydroxide to the chloride ion.

The conductivity and WU of these AEMs at 60 °C and room temperature were plotted as a function of the St content (**Figure 2**). The AEMs showed a steady decrease in conductivity from 89 to 70 mS/cm with increasing St content in a graft chain from 0% to 63%. The WU of AEMs also decreased slightly from 44% to 29% with increasing St content up to 63%. Interestingly, both the conductivity and WU of the AEMs increased suddenly and significantly (97 mS/cm and 52%, respectively) at a St content of 81%. Note that the chloride form of the VBA/St-AEM membranes, where the counter anion is Cl-, exhibited a similar trend (**Table S2**).

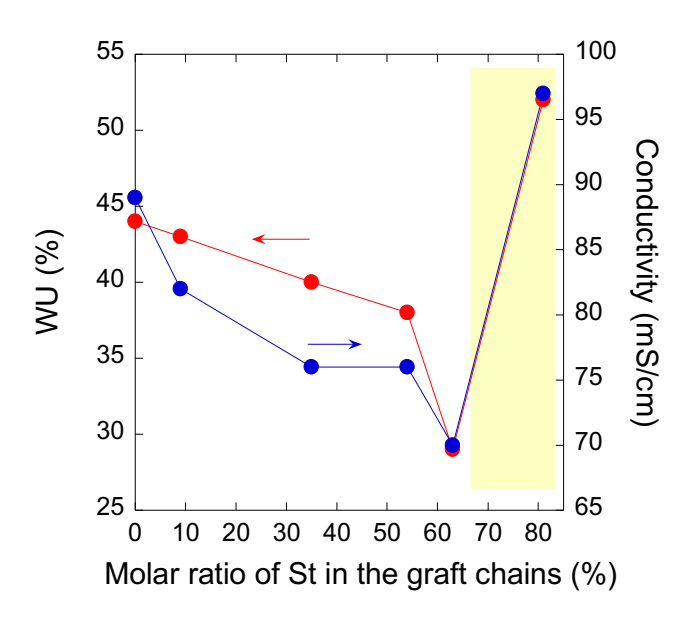


Figure 2. WU measured at 20 °C (red closed circle) and conductivities measured at 60 °C (blue closed circle) for VBA/St-AEM as a function of the molar ratio of St in the graft chains.

Generally, an increase in St content in a graft chain increases the hydrophobicity of the graft-polymer chain. Therefore, a suppressed conductivity and WU for the membranes appear rational. This was the case when the St content was less than 63%. However, further increases in St content showed an opposite result, which contravenes the typical correlations of the conductivity and WU with the hydrophobicity of the membranes. A random distribution of CMS and St in the graft component might prevent the separation of the two monomer units into hydrophilic and hydrophobic domains, leading to dilution and an increase in the hydrophilic region. This may be related to the increase in free volume by the introduction of more St groups, resulting in structural rearrangement of the ion channels.

2.3. Structural analysis on VBA/St-AEM with different St contents

The microscopic structures of these VBA/St-AEMs equilibrated in heavy water (D_2O) were compared using the SANS method to quantify the structural features as a function of the hydrophobicity of the membrane, which cannot be explained simply by the difference in the chemical structures of the AEM.¹⁴⁰⁻⁴²¹ The SANS intensity profiles, I(q), of these VBA/St-AEMs with different St contents equilibrated in D_2O were plotted as a function of the scattering vector, q, as shown in **Figure 3**.

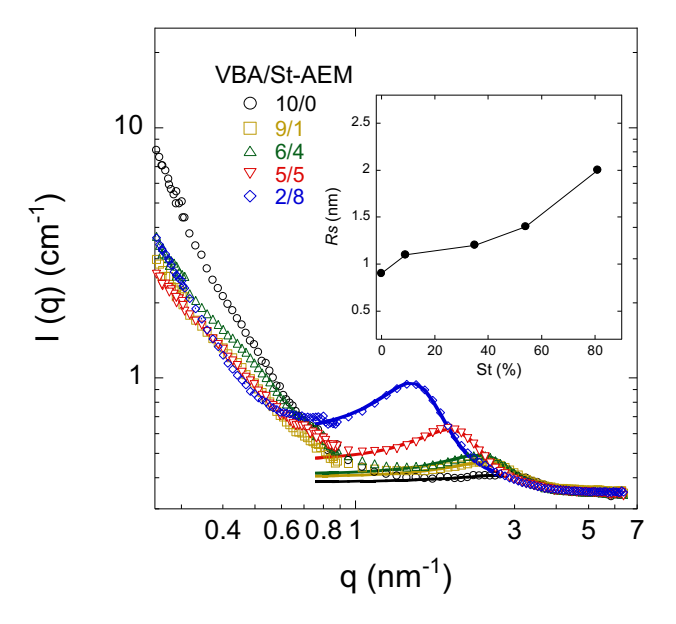


Figure 3. SANS profiles measured for VBA/St-AEM (10/0, 9/1, 6/4, 5/5, and 2/8) with different St contents equilibrated in D_2O at room temperature. The best-fitted theoretical solid lines based on hard-sphere (HS) liquid model analysis are also shown. Inset: St concentration dependence of R_1 obtained from the HS liquid model.

A previous study concluded that all the hydrated graft-type AEMs might have structural commonalities in that microphase separation between conducting and non-conducting phases based on the morphological features of the radiation-grafted AEMs with graft copolymers of 2-methyl-*N*-vinylimidazolium and styrene (2MNVIm/St-AEMs).^[41,63] In that system, the conducting phase was made from graft polymers and water. The non-conducting phase consisted of fluorinated base polymers and a small fraction of graft polymers embedded in the base polymers. This microphase separation was observed over the entire range of GDs and IECs of the graft-type AEMs. The length scale of the conducting/non-conducting phases depends on the original alternating crystalline/amorphous domains in the base polymers. In the ETFE-based graft-type AEMs, a broad peak originated from conducting/non-conducting microphase

separation at $q < 0.8 \text{ nm}^{-1}$ (real space, d = 8 nm). The d value shifted slightly to a longer distance with increasing GDs and IECs. In the SNAS profiles of graft-type AEMs, the GDs and IECs of the AEMs significantly affected the microstructures in the hydrophilic conducting phase on a length scale of 3-5 nm. Therefore, this study focused on structural analysis of the SANS profiles at q > 0.8 nm-1, as shown in **Figure 3**, and discussed the microstructures of VBA/St-AEM by comparing them with those of previously reported graft-type ETFE-based AEMs.

A clear scattering maximum at 1 nm⁻¹ < q < 4 nm⁻¹ was observed for all AEMs, which is the so-called ionomer peak, indicating the formation of ionic clusters in the presence of water. The peak position, q_m , shifted toward a small-q range, and the peak intensity, I_m , increased continuously with increasing St content. A similar phenomenon was observed in previous studies on 2MNVIm/St-AEMs when the St content (hydrophobicity) of the graft polymers was increased to more than 60%. [41,48] Therefore, a similar structural analysis was performed on the ionomer peak, assuming that the peak is related to the water-rich nano-domains like "water puddles" dispersed randomly and phase-separated from the homogeneous graft/water domains. The hard-sphere (HS) liquid model was used to fit the profiles. The theoretical curves were well fitted to the profiles at the higher q region, as shown by solid lines in Figure 3. Table 2 lists the average radius of the spherical water puddles (R) in the conducting regions from the best fitting results. The inset in **Figure 3** shows R, as a function of the St content. A steady increase in R_s was observed when the St content was less than 60%, and R_s then increased quickly. This indicates the tendency of the size change in water puddles. This ionomer peak was never observed in the dry AEMs, by either SANS or small-angle X-ray scattering techniques because of the poor contrast between the graft polymers and the ionic head.

In addition to the change in puddle size, more information on the water distribution over the entire membrane was also expected. Therefore, the exact volume fractions of water in puddles $(\phi_{w,puddle})$ and in other conducting layers with the graft polymers $(\phi_{w,graft})$ should be determined

quantitatively. When the sphere fraction of a water puddle (f_s) is defined as the ratio of $\phi_{w_{-puddle}}$ to the total volume fraction of the conducting phase (ϕ_{con}) , $\phi_{w_{-puddle}}$ can be expressed simply as Equation (1):

$$\phi_{\text{w puddle}} = f_{\text{s}} \times \phi_{\text{con}}$$
 (1)

 $\phi_{\text{\tiny con}}$ is the sum of the volume fractions of the graft polymers in the conducting phase ($\phi_{\text{\tiny con,graft}}$) and water ($\phi_{\text{\tiny w}}$), as follows:

$$\phi_{\rm con} = \phi_{\rm con_graft} + \phi_{\rm w}$$
 (2)

 ϕ_{w} is calculated using Equation (3):

$$\phi_w = \frac{\frac{WU/100(1 + GD/100)}{d_w}}{\frac{1}{d_{errfe}} + \frac{GD/100}{d_{graft}} + \frac{WU/100(1 + GD/100)}{d_w}}$$
(3)

where d_{eff} , d_{graft} , and d_{w} are the mass densities of ETFE base film, grafts, and water, being 1.7, 1.0, and 1.0 g/cm³, respectively. [40-43] Therefore, ϕ_{w} can be estimated in terms of GD and WU for each AEM, as listed in **Table 2**. This study took advantage of the fact that the volume ratio of conductive graft polymers to the total graft polymers ($\phi_{\text{con_graft}}/\phi_{\text{graft}}$) is close to the IEC_{cup}/IEC_{cul.} ratio to obtain the $\phi_{\text{con_graft}}$ values. According to **Table 1**, IEC_{cup}/IEC_{cul.} for all AEMs was ~0.8. Therefore, it can be reasonably assumed that

$$\phi_{\text{con_graft}} = 0.8 \times \phi_{\text{graft}}$$
 (4)

 ϕ_{gmft} is calculated using Equation (5).

$$\phi_{graft} = \frac{\frac{GD/100}{d_{graft}}}{\frac{1}{d_{ETFE}} + \frac{GD/100}{d_{graft}} + \frac{WU/100(1 + GD/100)}{d_{w}}}$$
(5)

Combining Equations (1)–(5), $\phi_{w\text{-puddle}}$ and $\phi_{w\text{-graft}}$ (= ϕ_{w} - $\phi_{w\text{-puddle}}$) can be estimated for each AEM, as listed in **Table 2**. The water distribution in the membranes can be visualized by plots of ϕ_{w} , $\phi_{w\text{-puddle}}$, and $\phi_{w\text{-graft}}$ as a function of the St content, as shown in **Figure 4**.

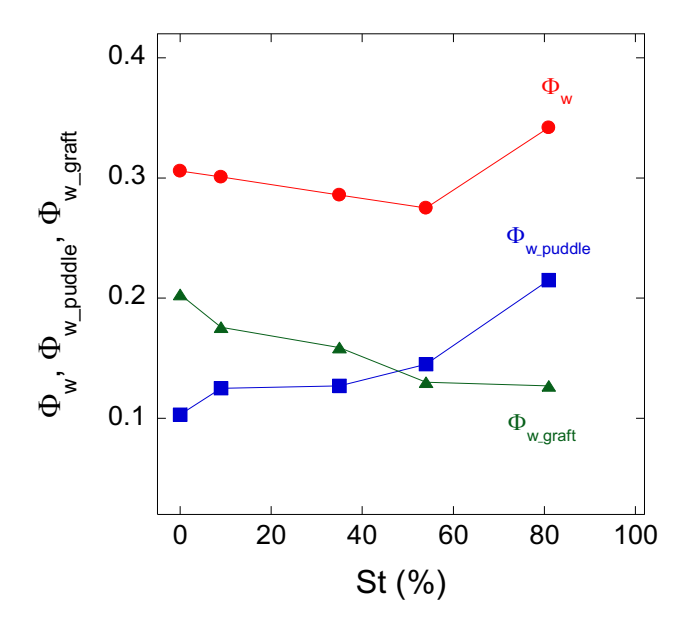


Figure 4. Plots of ϕ_{v} , $\phi_{v_{-produle}}$, and $\phi_{v_{-graft}}$ as a function of the St content.

According to the St content dependence of WU, ϕ_{w} decreased slightly from 0.31 to 0.28 (nearly constant) with increasing St content from 0% to 63% and then increased from 0.28 to

0.34 (~25% net increase) at St contents higher than 63%. Although the total water volume ϕ was relatively constant at St contents lower than 63%, two components, $\phi_{e-puble}$ and $\phi_{e-puble}$, increased and decreased with increasing St content, respectively, to cancel each other. The significant increase in ϕ with increasing St content from 63% to 81% appeared to result from only the increase in $\phi_{e-puble}$ (15–22%) but not $\phi_{e-puble}$ (13–13%). A previous study on 2MNVIm/St-AEMs revealed a homogeneous water distribution in graft polymers at St contents lower than 60%. However, the conducting phase in VBA/St-AEM caused phase separation of the heterogeneous water-puddle structures from the graft/water coordinate matrix, even for the VBA-AEM, which has no hydrophobic St unit. This is probably due to the strong basicity of ammonium hydroxide compared to the imidazolium group in 2MNVIm/St-AEMs, being capable of more water association in the membranes. The number density of water puddles (n_{puble}) in the AEM relevant to VBA-AEM (10/0) was estimated to determine how the water puddles associate with one another in the membrane as a function of the St content, as follows:

$$n_{\text{puddle}}/n_{\text{puddle},0} = \frac{\phi_{\text{w_puddle}} R_{s,0}^3}{\phi_{\text{wpuddle},0} R_s^3}$$
 (6)

where $n_{puddle0}$, R_{s0} , and $\phi_{e_{puddle0}}$ represent the number density, average radius, and volume fraction of the water puddles in VBA-AEM (10/0), respectively. The resulting $n_{puddle}/n_{puddle0}$ showed a continuous decrease with increasing St content (**Table 2**). $n_{puddle}/n_{puddle0}$ decreases to 0.2 when the St content was increased to 83%. This result shows that the water puddles may coalesce and grow larger with increasing St content, as illustrated in **Figure 5**.

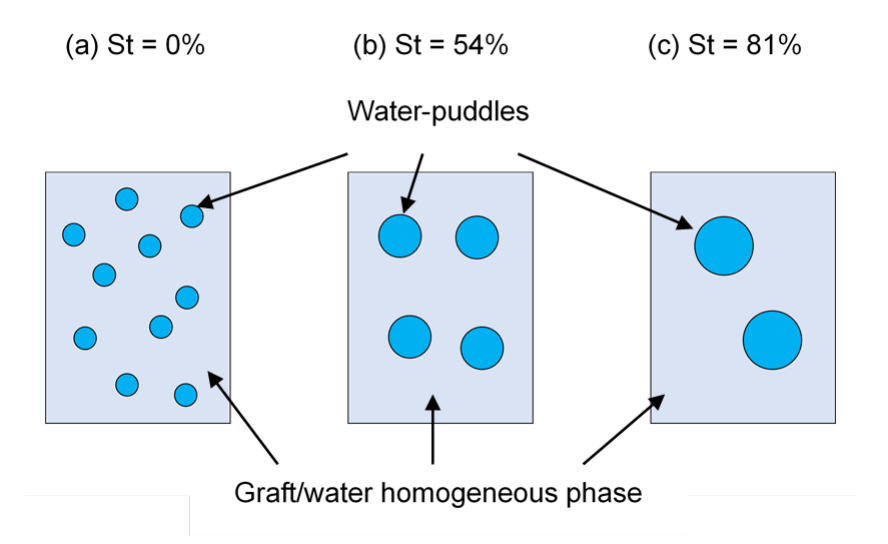


Figure 5. Illustrations of water puddles distributed in VBA/St-AEM with different St contents.

The enhancement of the ionomer peak with increasing St content is due mainly to the increase in the volume fraction of water puddles, as shown in **Figure 3**. The water distribution with the graft polymers ($\phi_{e_{graft}}$) decreased continuously because of the increase in hydrophobicity of the graft polymers, which is always true no matter how the heterogeneity of the matrix varies. The sudden increase in $\phi_{e_{graft}}$ at St contents > 60% was because the rapid increase in $\phi_{e_{graft}}$ outweighs the slight decrease in $\phi_{e_{graft}}$. According to a previous study, this was partially due to the stronger hydrophilic/hydrophobic segregation power between the graft polymers and water and partially due to the formation of an extra conducting phase made from graft polymers outside of the crystalline stacks because of the extremely high GD over 100%. This different grafting phase extends beyond the original semi-crystalline frames and behaves less constrained, which weakens the chemical and dimensional stabilities of the membrane and easily holds water.

2.4. Thermal and mechanical properties of graft-type AEMs

The effects of St on the thermal and mechanical properties of AEMs were examined by thermogravimetric analysis (TGA) and tensile testing. The chloride form of VBA-AEM and

VBA/St-AEMs was used because the hydroxide form of the AEM is converted easily to the bicarbonate form. The thermal and mechanical stabilities of AEMs with the chloride form are generally higher than those of the corresponding hydroxide forms but are relatively parallel. Hence, it is reasonable to discuss the effects of St on the thermal stability of the AEMs with the chloride forms. The chloride form of VBA-AEM with a calculated IEC₀ of 1.14 mmol/g showed a three-step degradation process (**Figure S1**). This is a similar profile to previous data of the chloride form of VBA-AEM.¹⁹³ The first weight loss was observed at approximately 202 °C (determined as the onset temperature by extrapolation) (**Table S3**). A previous study reported the decomposition mechanism of the chloride form of VBA-AEM by TGA-mass spectroscopy.¹⁹³ The first decomposition was assigned to the degradation of the ionic group, i.e., the elimination of TMA. The second and third weight losses observed at approximately 376 °C and 494 °C were assigned to the degradation of the graft polymers and the ETFE substrate, respectively.^{191,192,87}

The St-cografted VBA/St-AEM chloride form showed similar decomposition behavior to VBA-AEM except for the different ratios of weight losses between the ionic groups and graft polymers. The chloride form of VBA/St-AEM (5/5) with an IEC₀ of 1.02 mmol/g and VBA/St-AEM (2/8) with an IEC₀ of 0.96 mmol/g exhibited a lower decomposition temperature than the chloride form of VBA-AEM, despite its similar IEC. The first degradation temperature decreased from 199 °C to 178 °C with increasing St molar ratio in the graft chain, probably because of a change in the segmental motion of the graft chains. In particular, the low glass transition temperature of the polystyrene (PSt) units in the graft chains decreased the decomposition temperatures of the AEMs were also supported by derivative differential thermal analysis (DDTA) of the chloride form of VBA-AEM and VBA/St-AEM (Figure S2). The temperatures at the inflection point of the chloride form of VBA/St-AEM (203–229 °C) were lower than those of VBA-AEM (233–241 °C). Accordingly, the St units in the graft chain

affected the thermal stability of the graft-type AEMs. DDTA analysis provided information on the stability of ETFE base polymers. The temperature at the inflection points of VBA-AEM and VBA/St-AEMs at approximately 260 °C, which was attributed to the melting point of the ETFE units, was relatively constant, even by changing the GDs and the St contents. Hence, the introduction of PSt and ionic ammonium hydroxide group did not affect the ETFE. Therefore, the introduction of a PSt graft chain and ionic ammonium hydroxide group did not affect the thermal properties of the ETFE-based polymer units in the AEMs.

The tensile strength and the elongation at break of the chloride form of VBA-AEM with an IEC_a of 1.24 mmol/g and VBA/St-AEM (5/5) with an IEC_a of 1.25 mmol/g were measured under atmospheric conditions to understand the effects of St in the graft chain on the mechanical properties, which is one of the critical properties for preparing the membrane electrode assemblies and the long-term stability during fuel cell operation. The chloride form of VBA-AEM and VBA/St-AEM (5/5) showed high tensile strength (43 and 44 MPa, respectively) (**Table S4**). The chloride forms of VBA-AEM and VBA/St-AEM (5/5) exhibited elongation at breaks of 100% and 70%, respectively. Pure PSt has a relatively low elongation at break (<5%). The increases in the PSt unit in the graft chain decrease the elongation at break of the VBA/St-AEMs. The introduction of St in the graft chain decreased the elongation at break.

2.5. Alkaline stabilities of graft-type AEMs

The effects of hydrophobic St in the graft chain on the alkaline durability of the AEMs were evaluated by comparing the stabilities of VBA/St-AEM with VBA/St ratios of 5/5 and 4/6 and IECs of 0.84 and 0.85 mmol/g with a VBA-AEM with a similar IEC (0.97 mmol/g). As a metric of the alkaline stability, the changes in the conductivities of the AEMs in 1 M KOH at 80 °C were monitored and plotted as a function of the immersion time (h), as shown in **Figure 6**. The conductivity of VBA-AEM, which has no hydrophobic St unit in the grafts, decreased with increasing immersion time in a 1 M KOH solution at 80 °C and decreased to 60% of the initial

level at 720 h. In contrast, hydrophobic St cografted VBA/St-AEMs (5/5) and (4/6) maintained their initial conductivities, even after 720 h (**Figure 6**).

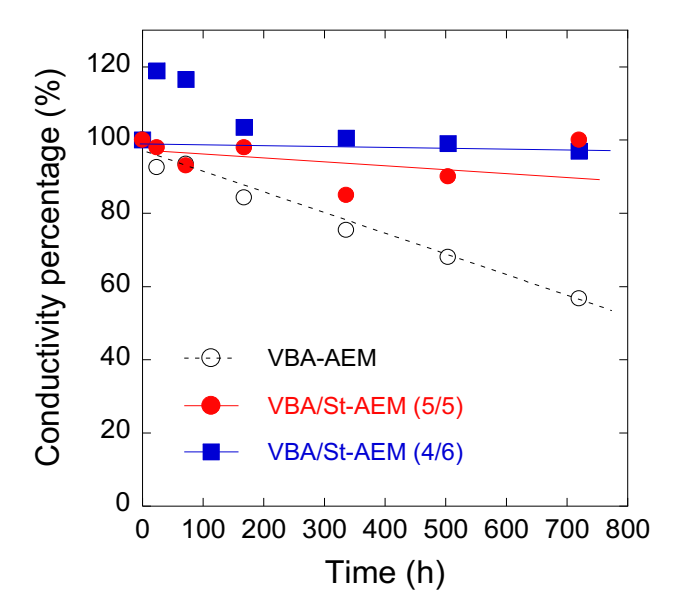


Figure 6. Time course of the conductivities of VBA-AEM with an IEC of 0.97 mmol/g (black open circles), VBA/St-AEM (5/5) with an IEC of 0.84 mmol/g (red closed circles), and VBA/St-AEM (4/6) with an IEC of 0.85 mmol/g (blue closed square) after immersion in a 1 M KOH aqueous solution at 80 °C, measured at 20 °C in nitrogen-saturated deionized water.

Table 3 lists the IECs of the tested AEMs after the 720 h alkaline stability test. The IEC of VBA-AEM retained 64% of the initial IEC value. The AEMs with higher St contents in the grafts retained higher initial IEC values, i.e., VBA/St-AEMs (5/5) and (4/6) exhibited IECs with initial values of 83 and 89%, respectively. Accordingly, the hydrophobic St units in the graft chain improved the alkaline stability. They suppressed the degradation of the anion-conducting group (ammonium cation) of the graft-type AEMs, resulting in improved alkaline stability. This is a similar effect to the alkyl-substituents on ammonium group and alkyl spacer between the polymer backbone and the ammonium group, as mentioned in the introduction.^[25-27]

Similar to monitoring the IECs of the post samples after the alkaline stability test for 720 h, the effects of St in the graft chain on the mechanical properties of graft-type AEMs under alkaline conditions was examined (**Table S4**). VBA-AEM with an IEC_a of 1.24 mmol/g and VBA/St-AEM (5/5) with an IEC_α of 1.25 mmol/g were converted from the hydroxide to chloride form by immersion in 0.5 M hydrochloric acid for five days before measuring the tensile strength and elongation at break. The tensile strength of the chloride form of VBA-AEM and VBA/St-AEM (5/5) decreased from 43 and 44 MPa to 18 and 21 MPa, respectively, in 1 M KOH at 80 °C for 720 h. These values were less than 50% of the initial levels. The elongation at break also decreased to 11% and 6% of the initial values, respectively. Unfortunately, the mechanical properties of VBA/St-AEM (5/5) decreased in 1 M KOH at 80 °C. Recently, 4vinylimidazolium/styrene-cografted AEMs were also reported to show decreases in tensile strength to 63% of the initial level in 1 M KOH at 80 °C for 24 h.47 In contrast to the effects on the IEC changes, the introduction of hydrophobic St units in the grafts had no positive effect on enhancing the mechanical properties of the AEMs in alkaline environments, suggesting degradation with a structural change in the base polymer ETFE in an alkaline solution at high temperatures.

The degradation mechanism of the graft-type AEM in an alkaline solution at the molecular level was examined by observing the structural changes to VBA-AEM with an IEC_a of 1.24 mmol/g and VBA/St-AEM (5/5) with an IEC_a of 1.25 mmol/g before and after the alkaline stability test for 720 h by FT-IR spectroscopy using the potassium bromide method (**Figure 7**). The chloride forms were used for FT-IR analysis because of the stability of the AEMs, as mentioned in the previous section. For VBA-AEM, the intensity of the absorbance at approximately 1490 cm⁻¹, corresponding to the quaternized ammonium group, decreased. The absorbance corresponding to the quaternized ammonium group of the post-tested VBA/St-AEM (5/5) showed a slight decrease. These results are in good agreement with the IEC changes after the alkaline stability test, i.e., the decreases in IECs and conductivities of the AEMs were

attributed to the degradation of the quaternized ammonium group, similar to the conventional degradation manner (**Figure 8**). The St in the graft chain suppressed the attack of the hydroxide anion and enhanced the alkaline stability.

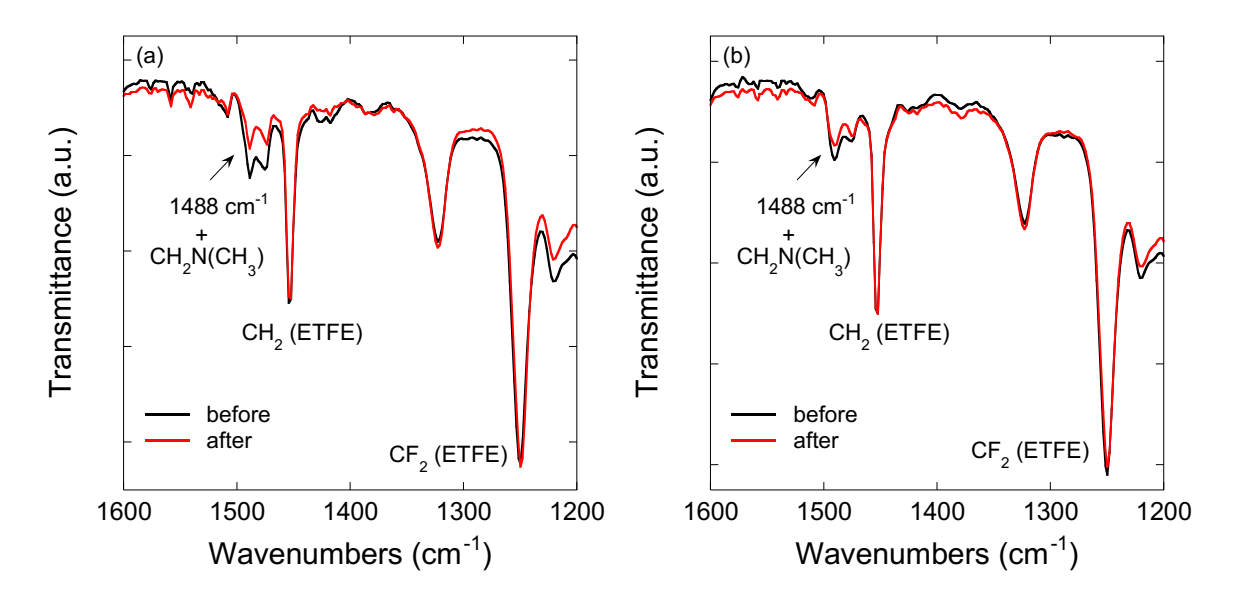


Figure 7. FT-IR spectra of the (a) chloride form of VBA-AEM with an IEC_a of 1.24 mmol/g and (b) chloride form of VBA/St-AEM (5/5) with an IEC_a of 1.25 mmol/g before and after immersion in 1 M KOH at 80 °C for 720 h.

Figure 8. Proposed degradation mechanism of the graft-type AEM in 1 M KOH at 80 °C.

The decreases in the tensile strength and elongation at break might be due to the decomposition of ETFE by the attack of hydroxide ions in VBA-AEM, which is a strong base, even though no spectral changes in ETFE were not observed in the FT-IR spectrum after immersion in 1 M KOH at 80 °C for 720 h. Pristine ETFE, which exhibits a tensile strength of 53 MPa and elongation at breaks of 103%, was stable in a 1 M KOH solution at 80 °C for 720 h with no changes in the mechanical properties (**Table S4**). One explanation for the above stability of ETFE under alkaline conditions is that the polymer chains of ETFE were stable under the above alkaline stability test conditions for at least a few days. On the other hand, they were unstable in the hydrated graft-polymer phase containing tetraalkylammonium hydroxide, which is one of the strongest organic bases, at 80 °C.

The following tests support this hypothesis. Even in pure water at 80 °C, VBA-AEM with an IEC of 1.54 mmol/g exhibited similar degradation behavior to that observed in 1 M KOH. Although there was no change in conductivity, the tensile strength of the chloride form of VBA-AEM decreased from 47 to 38 MPa (19% decrease). In particular, the elongation at break decreased drastically from 78 to 44% (44% decline) for only 12 h. The ETFE base polymers in the AEMs were decomposed by the attack of hydroxide ions, as observed in the other fluorinated PEMs, i.e., the elimination reaction of hydrogen fluoride (HF) molecules, because graft chain decomposition and ETFE were not observed in the ¹³C solid-state NMR and FT-IR spectra. ^{148,89}

3. Conclusion

VBA/St-AEMs with similar IECs of 0.78–1.06 mmol/g were prepared by the radiation-induced graft polymerization of CMS with hydrophobic St as the comonomer and successive quaternization and anion-exchange reactions for assessing the influence of the hydrophobicity of the graft chain on the conductivity, WU, and alkaline stability. Increasing the molar ratio of

St in the graft chain from 0% to 63% resulted in a 21% and 34% decrease in conductivity and WU of VBA/St-AEM, respectively. On the other hand, the AEM with an 81% molar ratio of St exhibited 9% and 18% higher conductivity and WU, respectively, than the non-St-cografted one. SANS analysis showed that this phenomenon was due to the formation of water-rich nanodomains like "water puddles" dispersed randomly and phase-separated homogeneous graft chain/water domains. TGA revealed a decrease in the degradation temperature of the chloride form of VBA/St-AEM with increasing St molar ratio in the graft chain.

In the alkaline durability test of VBA/St-AEM in 1 M KOH at 80 °C for 720 h, the loss of conductivity was suppressed from 43% to 8% at the initial level because of the remaining IEC from 36% to 11% when the St contents in the grafts were increased from 0% to 63%. This suggests that hydrophobic St in the graft chain has a positive effect on the alkaline stability of the graft-type AEM. In contrast, the tensile strength and elongation at break of the AEM decreased to approximately 50% and 10% of the initial value, respectively. The hydrophobic St in the graft chain improved the alkaline stability, but St had no effects on the mechanical properties. The decomposition of ETFE by the attack of hydroxide ions, i.e., the elimination reaction of HF molecules, similar to the dehydrofluorination in polyvinylidene difluoride, might occur in 1 M KOH at 80 °C. Overall, these findings will be useful for the further design and synthesis of AEMs.

Supporting Information Summary

The experimental procedures for the synthesis and characterization of VBA/St-AEMs are provided in the Supporting Information.

Acknowledgments

This study was supported partially by the Advanced Low Carbon Technology Research and Development Program (ALCA) from the Japan Science and Technology Agency (JST) and

Grant-in-Aid for Scientific Research (A) from the Japan Society for the Promotion of Science

(JSPS) (KAKENHI Grant Number: 18H03850). The authors wish to thank Enago for the

English language review.

Author Contributions

The manuscript was written through the contributions of all authors. All authors have

approved the final version of the manuscript. Individual author contributions are as follows:

T.H. designed the research, contributed to all of the experimental work, and wrote the paper.

Y.Z., K.Y., A.R., and K.O. contributed to the SANS measurement. Y.Z. analyzed the SANS

data. Y.M. directed this study and edited the paper.

Conflict of Interest

The authors declare no conflict of interest.

Keywords: Alkaline durability · Anion-conducting electrolyte membrane · Poly(ethylene-co-

tetrafluoroethylene) · Radiation-induced graft polymerization · Small-angle neutron scattering

Received: ((will be filled in by the editorial staff))

Revised: ((will be filled in by the editorial staff))

Published online: ((will be filled in by the editorial staff))

References

D. R. Dekel, J. Power Sources 2018, 375, 158-169. [1]

[2] S. Gottesfeld, D. R. Dekel, M. Page, C. Bae, Y. Yan, P. Zelenay, Y. S. Kim, J. Power

Sources 2018, 375, 170-184.

23

- [3] L. Wang, T. Weissbach, R. Reissner, A. Ansar, A. S. Gago, S. Holdcroft, K. A. Friedrich, *ACS Appl. Energy Mater.* **2019**, 2, 7903-7912.
- [4] X. Gao, L. He, H. Yu, F. Xie, Y. Yang, Z. Shao, *Int. J. Hydrog. Energy* **2020**, *45*, 23353-23367.
- [5] J. Cheng, G. He, F. Zhang, *Int. J. Hydrog. Energy* **2015**, *40*, 7348-7360.
- [6] F. H. Liu, C. X. Lin, E. N. Hu, Q. Yang, Q. G. Zhang, A.M. Zhu, Q. L. Liu, J. Membr. Sci. 2018, 564, 298-307.
- [7] Z. G. Abdi, T.-H. Chiu, Y.-Z. Pan, J.-C. Chen, *React. Funct. Polym.* **2020**, *156*, 104719.
- [8] J. Wang, Z. Zhao, F. Gong, S. Li, S. Zhang, *Macromolecules* **2009**, *42*, 8711-8717.
- [9] S. D. Poynton, R. C. T. Slade, T. J. Omasta, W. E. Mustain, R. Escudero-Cid, P. Ocón,
 J. R. Varcoe, J. Mater. Chem. A 2014, 2, 5124-5130.
- [10] C. M. Tuan, D. Kim, J. Membr. Sci. 2016, 511, 143-150.
- [11] O. M. M. Page, S. D. Poynton, S. Murphy, A. L. Ong, D. M. Hillman, C. A. Hancock,M. G. Hale, D. C. Apperley, J. R. Varcoe, RSC Advances 2013, 3, 579-587.
- [12] B. Lin, H. Dong, Y. Li, Z. Si, F. Gu, F. Yan, Chem. Mater. 2013, 25, 1858-1867.
- [13] Z. Si, L. Qiu, H. Dong, F. Gu, Y. Li, F. Yan, *ACS Appl. Mater. Interfaces* **2014**, *6*, 4346-4355.
- [14] D. D. Tham, D. Kim, J. Membr. Sci. **2019**, 581, 139-149.
- [15] K. Yang, H. Ni, T. Shui, X. Chi, W. Chen, Q. Liu, J. Xu, Z. Wang, *Polymer* 2020, 211, 123085.
- [16] G. Merle, M. Wessling, K. Nijmeijer, *J. Membr. Sci.* **2011**, *377*, 1-35.

- [17] K. M. Meek, J. R. Nykaza, Y. A. Elabd, *Macromolecules* **2016**, *49*, 3382-3394.
- [18] Y. Ye, Y. A. Elabd, *Macromolecules* **2011**, *44*, 8494-8503.
- [19] J. R. Varcoe, P. Atanassov, D. R. Dekel, A. M. Herring, M. A. Hickner, P. A. Kohl, A. R. Kucernak, W. E. Mustain, K. Nijmeijer, K. Scott, T. Xu, L. Zhuang, *Energy Environ. Sci.* **2014**, *7*, 3135-3191.
- [20] K. M. Hugar, H. A. Kostalik, IV, G. W. Coates, J. Am. Chem. Soc. 2015, 137, 8730-8737.
- [21] M. Tanaka, M. Koike, K. Miyatake, M. Watanabe, *Polym. Chem.* **2011**, 2, 99-106.
- [22] C. Fujimoto, D.-S. Kim, M. Hibbs, D. Wrobleski, Y. S. Kim, *J. Membr. Sci.* **2012**, *423*-424, 438-449.
- [23] A. Amel, L. Zhu, M. Hickner, Y. Ein-Eli, J. Electrochem. Soc. **2014**, 161, F615-F621.
- [24] Y.-K. Choe, C. Fujimoto, K.-S. Lee, L. T. Dalton, K. Ayers, N. J. Henson, Y. S. Kim, *Chem. Mater.* **2014**, *26*, 5675-5682.
- [25] M. R. Hibbs, J. Polym. Sci., Part B: Polym. Phys. 2013, 51, 1736-1742.
- [26] X. Du, H. Zhang, Y. Yuan, Z. Wang, J. Xu, Int. J. Hydrog. Energy 2020, 45, 11814-11823.
- [27] A. D. Mohanty, C. Y. Ryu, Y.S. Kim, C. Bae, *Macromolecules* **2015**, *48*, 7085-7095.
- [28] J. Chen, D. Li, H. Koshikawa, M. Zhai, M. Asano, H. Oku, Y. Maekawa, *J. Membr. Sci.* **2009**, *344*, 266-274.
- [29] S. Hasegawa, S. Takahashi, H. Iwase, S. Koizumi, N. Morishita, K. Sato, T. Narita, M. Ohnuma, Y. Maekawa, *Polymer* **2011**, *52*, 98-106.

- [30] S. Hasegawa, S. Takahashi, H. Iwase, S. Koizumi, M. Ohnuma, Y. Maekawa, *Polymer* **2013**, *54*, 2895-2900.
- [31] T. T. Duy, S. Sawada, S. Hasegawa, Y. Katsumura, Y. Maekawa, *J. Membr. Sci.* **2013**, 447, 19-25.
- [32] T. Hamada, S. Hasegawa, H. Fukasawa, S. Sawada, H. Koshikawa, A. Miyashita, Y. Maekawa, J. Mater. Chem. A 2015, 3, 20983-20991.
- [33] T. Hamada, H. Fukasawa, S. Hasegawa, A. Miyashita, Y. Maekawa, *Int. J. Hydrog*. *Energy* **2016**, *41*, 18621-18630.
- [34] T. Hamada, S. Hasegawa, Y. Maekawa, *Macromol. Chem. Phys.* **2017**, 218, 1700346.
- [35] H. Koshikawa, K. Yoshimura, W. Sinnananchi, T. Yamaki, M. Asano, K. Yamamoto,
 S. Yamaguchi, H. Tanaka, Y. Maekawa, *Macromol. Chem. Phys.* 2013, 214, 1756-1762.
- [36] K. Yoshimura, H. Koshikawa, T. Yamaki, H. Shishitani, K. Yamamoto, S. Yamaguchi, H. Tanaka, and Y. Maekawa, *J. Electrochem. Soc.* **2014**, *161*, F889-F893.
- [37] T. Hamada, K. Yoshimura, A. Hiroki, Y. Maekawa, J. Appl. Polym. Sci. 2018, 135, 46886.
- [38] K. Yoshimura, A. Hiroki, H.-C. Yu, Y. Zhao, H. Shishitani, S. Yamaguchi, H. Tanaka, Y. Maekawa, *J. Membr. Sci.* **2019**, *573*, 403-410.
- [39] B.-S. Ko, J.-Y. Sohn, J. Shin, *Polymer* **2012**, *53*, 4652-4661.
- [40] Y. Zhao, K. Yoshimura, H. Shishitani, S. Yamaguchi, H. Tanaka, S. Koizumi, N. Szekely, A. Radulescu, D. Richter, Y. Maekawa, *Soft Matter* **2016**, *12*, 1567-1578.

- [41] K. Yoshimura, Y. Zhao, A. Hiroki, Y. Kishiyama, H. Shishitani, S. Yamaguchi, H. Tanaka, S. Koizumi, J. E. Houston, A. Radulescu, M.-S. Appavou, D. Richter, Y. Maekawa, *Soft Matter* **2018**, *14*, 9118-9131.
- [42] Y. Zhao, K. Yoshimura, H.-C. Yu, Y. Maekawa, A. Hiroki, Y. Kishiyama, H. Shishitani, S. Yamaguchi, H. Tanaka, S. Koizumi, M.-S. Appavou, J. Houston, A. Radulescu, and D. Richter, *Physica B: Condens. Matter* **2018**, *551*, 203-207.
- [43] K. Yoshimura, Y. Zhao, S. Hasegawa, A. Hiroki, Y. Kishiyama, H. Shishitani, S. Yamaguchi, H. Tanaka, S. Koizumi, M.-S. Appavou, A. Radulescu, D. Richter, Y. Maekawa, *Soft Matter* **2017**, *13*, 8463-8473.
- [44] T. D. Tap, S. Sawada, S. Hasegawa, K. Yoshimura, Y. Oba, M. Ohnuma, Y. Katsumura, Y. Maekawa, *Macromolecules* **2014**, *47*, 2373-2383.
- [45] M. M. Nasef, H. Saidi, K. Z. M. Dahlan, Radiat. Phys. Chem. 2003, 68, 875-883.
- [46] S. A. Gürsel, J. Schneider, H. B. youcef, A. Wokaun, G. G. Scherer, *J. Appl. Polym. Sci.* **2008**, *108*, 3577-3585.
- [47] T. Hamada, K. Yoshimura, K. Takeuchi, S. Watanabe, Y. Zhao, A. Hiroki, T. Hagiwara, H. Shishitani, S. Yamaguchi, H. Tanaka, A. Radulescu, K. Ohwada, Y. Maekawa, *Macromol. Chem. Phys.* **2021**, 222, 2100028.
- [48] D. M. Brewis, I. Mathieson, I. Sutherland, R. A. Cayless, R. H. Dahm, *Int. J. Adhes. Adhes.* **1996**, *16*, 87-95.
- [49] Z. Xu, L. Li, F. Wu, S. Tan, Z. Zhang, J. Membr. Sci. 2005, 255, 125-131.

Table 1. GD, anion exchange, experimental and calculated IECs, conductivities, and WU of VBA-AEM and VBA/St-AEM

Entry	GD (%)	Molar ratio in the graft chain		Anion exchange	IECexp. (mmol/g)	IECcal. (mmol/g)	Conductivity (mS/cm)		WU (%)
		CMS	St	- (%)	(IIIIIo II g)	(11111011'g)	20 °C	60 °C	. (10)
VBA-AEM	24	100	0	84	0.97	1.16	55	89	44
VBA/St-AEM (9/1)	31	91	9	77	1.06	1.37	53	82	43
VBA/St-AEM (6/4)	30	65	35	79	0.83	1.05	45	76	40
VBA/St-AEM (5/5)	43	46	54	81	0.84	1.04	52	76	38
VBA/St-AEM (4/6)	50	37	63	89	0.85	0.96	47	70	29
VBA/St-AEM (2/8)	153	19	81	80	0.78	0.98	59	97	52

Table 2. Parameters from water-puddle model analysis for the AEMs equilibrated in water

Entry	R_{s} (nm)	$f_{\scriptscriptstyle \mathrm{s}}$	$oldsymbol{\phi}_{\!\scriptscriptstyle\mathrm{w}}$	$oldsymbol{\phi}_{ ext{ iny puddle}}$	$oldsymbol{\phi}_{ ext{ iny graft}}$	$n_{ ext{ iny puddle}}/n_{ ext{ iny puddle},0}$
VBA-AEM (10/0)	0.9	0.21	0.306	0.103	0.203	1
VBA/St-AEM (9/1)	1.1	0.24	0.301	0.125	0.176	0.66
VBA/St-AEM (6/4)	1.2	0.25	0.286	0.127	0.159	0.52
VBA/St-AEM (5/5)	1.4	0.26	0.275	0.145	0.13	0.37
VBA/St-AEM (2/8)	2.0	0.28	0.342	0.215	0.127	0.19

Table 3. Molar ratio of CMS and St in the graft chain and the decrease in IEC values for VBA-AEM and VBA/St-AEM after immersion in 1 M KOH at 80 °C

	GD (%)	Molar ratio of CMS/St	IEC (mmol/g)		Decline (%)
	GD (10)	in the graft chain	0 h	720 h	Decimie (%)
VBA-AEM (10/0)	24	100/0	0.97	0.62	36
VBA/St-AEM (5/5)	43	46/54	0.84	0.70	17
VBA/St-AEM (4/6)	50	37/63	0.85	0.76	11

Table of Contents (ToC)

Hydrophobic Effect on Alkaline Stability of Graft Chains in Ammonium-type Anion Exchange Membranes Prepared by Radiation-Induced Graft Polymerization

T. Hamada,* Y. Zhao, K. Yoshimura, A. Radulescu, K. Ohwada and Y. Maekawa*

Vinylbenzyltrimethylammonium hydroxide and styrene cografted poly(ethylene-cotetrafluoroethylene) anion exchange membranes (VBA/St-AEM) were prepared. The conductivity and water uptake of VBA/St-AEM decreased with increasing styrene content in the range of 0-63%. However, VBA/St-AEM with the 81% molar ratio of styrene exhibited higher conductivity and water uptake. The hydrophobic styrene in the graft chain enhanced the alkaline stability of VBA/St-AEM.

Graft-type Anion Exchange membrane

